Eur Biophys J (2008) 37:153–164
DOI 10.1007/s00249-007-0205-8

ORIGINAL PAPER

Role of ionization of the phosphate cosubstrate on phosphorolysis by purine nucleoside phosphorylase (PNP) of bacterial (*E. coli*) and mammalian (human) origin

Anna Modrak-Wójcik · Aneta Kirilenko · David Shugar · Borys Kierdaszuk

Received: 20 January 2007 / Revised: 31 May 2007 / Accepted: 12 June 2007 / Published online: 17 July 2007

Abstract Kinetics of the reactions of purine nucleoside phosphorylases (PNP) from *E. coli* (PNP-I, the product of the *deoD* gene) and human erythrocytes with their natural substrates guanosine (Guo), inosine (Ino), a substrate analogue N(7)-methylguanosine (m^7Guo), and orthophosphate (P_i, natural cosubstrate) and its thiophosphate analogue (SP_i), found to be a weak cosubstrate, have been studied in the pH range 5–8. In this pH range Guo and Ino exist predominantly in the neutral forms (pK_a 9.2 and 8.8); m^7Guo consists of an equilibrium mixture of the cationic and zwitterionic forms (pK_a 7.0); and P_i and SP_i exhibit equilibria between monoanionic and dianionic forms (pK_a 6.7 and 5.4, respectively). The phosphorolysis of m^7Guo (at saturated concentration) with both enzymes exhibits Michaelis kinetics with SP_i, independently of pH. With P_i, the human enzyme shows Michaelis kinetics only at pH ~5. However, in the pH range 5–8 for the bacterial enzyme, and 6–8 for the human enzyme, enzyme kinetics with P_i are best described by a model with high- and low-affinity states of the enzymes, denoted as enzyme-substrate complexes with one or two active sites occupied by P_i, characterized by two sets of enzyme-substrate dissociation constants (apparent Michaelis constants, K_{m1} and K_{m2}) and apparent maximal velocities (V_{max1} and V_{max2}). Their values, obtained from non-linear least-squares fittings of the Adair equation, were typical for negative cooperativity of both substrate binding ($K_{m1} < K_{m2}$) and enzyme kinetics ($V_{max1}/K_{m1} > V_{max2}/K_{m2}$). Comparison of the pH-dependence of the substrate properties of P_i versus SP_i points to both monoanionic and dianionic forms of P_i as substrates, with a marked preference for the dianionic species in the pH range 5–8, where the population of the P_i dianion varies from 2 to 95%, reflected by enzyme efficiency three orders of magnitude higher at pH 8 than that at pH 5. This is accompanied by an increase in negative cooperativity, characterized by a decrease in the Hill coefficient from n_H ~1 to n_H ~0.7 for Guo with the human enzyme, and to n_H ~0.7 and 0.5 for m^7Guo with the *E. coli* and human enzymes, respectively. Possible mechanisms of cooperativity are proposed. Attention is drawn to the substrate properties of SP_i in relation to its structure.

Keywords Purine nucleoside phosphorylase · Phosphate · Thiophosphate · Ionic forms · Enzyme kinetics · pH effects

Abbreviations

PNP	Purine nucleoside phosphorylase
PNP-I and PNP-II	PNPs from *E. coli*, the products of the *deoD* and *xapA* genes, respectively
m^7Guo	N(7)-methylguanosine
FA	Formycin A
m^6FA	N(6)-methylformycin A
m^7FA	N(7)-methylformycin A
Hepes	N-2-hydroxyethylpiperazine-N′-2-ethanesulfonic acid

A. Modrak-Wójcik · A. Kirilenko · D. Shugar · B. Kierdaszuk (✉)
Department of Biophysics, Institute of Experimental Physics, University of Warsaw, 93 Zwirki Wigury St, 02-089 Warsaw, Poland
e-mail: borys@biogeo.uw.edu.pl

D. Shugar
Institute of Biochemistry and Biophysics, Polish Academy of Sciences, 5a Pawinskiego St, 02-106 Warsaw, Poland

Mes	2-[N-morpholino]ethanesulfonic acid
P_i	Orthophosphate
SP_i	Thiophosphate

Introduction

The ubiquitous purine nucleoside phosphorylase (PNP, purine nucleoside:ortho-phosphate ribosyl transferase, EC 2.4.2.1.), a key enzyme of the salvage pathways of purine nucleosides, catalyses the reversible cleavage of the glycosidic bond of ribo- and 2′-deoxyribonucleosides of guanine and hypoxanthine in higher organisms, as well as of adenine in some prokaryotes, e.g. *E. coli* and *S. typhimurium*, as follows:

$$\beta\text{-nucleoside} + P_i \leftrightarrow \text{purine base} + \alpha\text{-D-pentose-1-phosphate}$$

The intrinsic role of these enzymes in the functioning of various organisms is well established, and, e.g. PNP-deficiency in humans results in impairment of T-cell function, and is usually fatal. Practical applications of these enzymes include tumour-directed gene therapy, development of clinical methods for treatment of PNP-deficiency, chemotherapeutic applications of inhibitors as selective immunosuppressive agents to suppress the host versus graft response in organ transplantation, potentiation by inhibitors of the antitumour and antiviral activities of various nucleoside analogues. This has stimulated extensive structural and kinetic analyses of the enzymes from various sources, and partial elucidation of the reaction mechanisms, including development of transition state analogues (Taylor Ringia and Schramm 2006), the most potent known inhibitors. The field has been frequently reviewed, the most recent, dealing with the enzymes from a wide variety of sources, being those of Bzowska et al. (2000), and Pugmire and Ealick (2002).

In contrast to mammalian organisms, *E. coli* has two PNPs denoted as PNP-I and PNP-II, which differ in substrate specificity. PNP-I, the product of the *deoD* gene, is a homohexameric enzyme active towards both 6-oxo and 6-amino purine nucleosides (Jensen 1976; Doskocil and Holy 1977), but not 2-oxo, e.g. xanthosine (Stoychev et al. 2002). In contrast, PNP-II, the product of the *xapA* gene, is a homotrimer active only against 6-oxopurine nucleosides, including xanthosine, and some analogues (Dandanell et al. 2005). The enzyme investigated in this study is *E. coli* PNP-I, hereafter referred to simply as PNP-I, but appended also are some observations on the corresponding behaviour of PNP-II.

A characteristic feature of PNPs from various sources is the non-Michaelis kinetics for some substrates, not due to an association/dissociation equilibrium between enzyme subunits, shown to be absent in the case of PNP-I from *E. coli* (Modrak-Wójcik et al. 2006) and calf spleen (Behlke et al. 2005). Consequently, it may be interpreted either as a result of cooperativity between substrate binding sites or of their heterogeneity. Such behaviour has been observed for the cosubstrate P_i with the PNP from human erythrocytes (Choi et al. 1986), calf-spleen (Ropp and Traut 1991), PNP-I (Jensen 1976), and *Cellulomonas* sp. (Wielgus-Kutrowska et al. 1998).

In the case of PNP-I, fluorescence studies on P_i binding at pH 7.6 pointed to the existence of two different types of binding sites, and/or two different enzyme states, with different affinities for P_i, and dissociation constants of 29 μM and 1.1 mM (Kierdaszuk et al. 1997). Relevant to this is the crystal structure of PNP-I (Koellner et al. 2002) showing that the enzyme is a trimer of dimers containing pairs of unsymmetrical active sites on each dimer.

Particularly interesting is the influence of the concentration of P_i on the affinity of the enzyme for some inhibitors, e.g. bisubstrate analogue inhibitors, including acyclovir diphosphate (Tuttle and Krenitsky 1984), nucleotide analogue inhibitors (Krenitsky et al. 1990) and antiviral acyclic nucleoside phosphonates (Kulikowska et al. 1998), which simultaneously interact with the binding sites for both nucleoside and phosphate. The K_i values for such inhibitors are markedly dependent on the P_i concentration, frequently being more effective at the low mM P_i concentration prevailing in human cells (Traut 1994), and explained by the existence of two states of the enzyme with different affinities for P_i, e.g. in the case of PNP-I (Kierdaszuk et al. 1997).

Worthy of note is the effect of P_i on the interaction of PNP-I with some specific inhibitors, e.g. the fluorescent formycin A (FA), a structural analogue of adenosine, and its N-methyl analogues, determined with the aid of steady-state and time-resolved fluorescence (Kierdaszuk et al. 2000) and phosphorescence spectroscopy (Wlodarczyk et al. 2004). FA in aqueous medium is an 85:15 equilibrium mixture of the N(1)-H and N(2)-H prototropic tautomers (Fig. 1) and the two tautomeric forms differ in emission properties (Wierzchowski and Shugar 1982). Interaction of FA with PNP-I led to selective binding of the N(2)-H form, i.e. a shift of the tautomeric equilibrium in favour of the latter, independent of P_i. But affinity of the ligand for the enzyme was enhanced in the presence of P_i (Kierdaszuk et al. 2000; Wlodarczyk et al. 2004).

With the more potent inhibitor N(6)-methyl-FA (m^6FA, a structural analogue of 1-methyladenosine), the amino-imino equilibrium of free m^6FA (Fig. 1) was shifted, on interaction with the enzyme in the absence of P_i, to

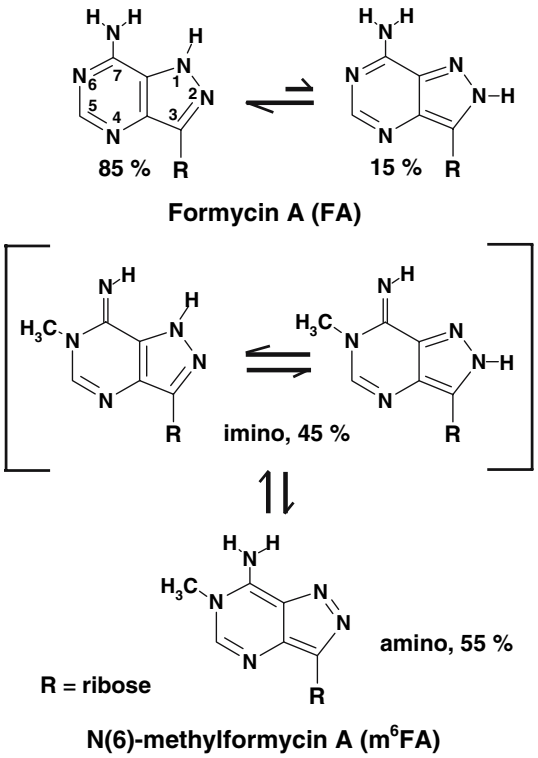

Fig. 1 Tautomerism of neutral forms of formycin A (FA) and N(6)-methylformycin A (m^6FA). Note that the imino form of m^6FA consists of an equilibrium mixture of two prototropic forms, N(1)-H and N(2)-H, the proportions of which are not known

selective binding of the imino species. In striking contrast, addition of P_i led to selective binding of the amino species, and a higher affinity for the enzyme, characterized by a 100-fold lower dissociation constant of the enzyme–ligand complex (Kierdaszuk et al. 2000). This is, in fact, a good example of identification of the tautomeric forms of protein-bound ligands, not distinguishable in X-ray studies (Koellner et al. 2002; Bzowska et al. 2005), where unambiguous determination of protons is limited by the resolution attainable.

In contrast to *E. coli* PNP-I (Kierdaszuk et al. 1997), two distinct binding modes of P_i in the complex with human PNP, although asymmetric (Deng et al. 2004), occur with similar affinities (Deng et al. 2006). They may be discriminated by the finding that a hydrogen bond to one PO group is stronger than those to the other two PO groups in one form of the PNP–P_i complex. In the light of studies by Deng et al. (2006), the two forms of bound P_i in the PNP–P_i complex are interpreted to be P_i positioned as the product in the nucleoside synthesis direction and as the substrate in the phosphorolysis reaction.

Less attention has hitherto been devoted to the role of P_i in the mechanism of PNP-I from *E. coli*. We have, consequently, extended earlier findings (Kierdaszuk et al. 1997) to a comparison of enzyme kinetics with respect to P_i for two PNPs with different specificities for their nucleoside substrates, as well as the effects of pH to determine the ionic species of P_i involved in the phosphorolytic pathway. To this end, we have also examined the behaviour of the phosphate analogue, thiophosphate (SP_i), which we initially found to be a weak competitor of P_i.

Experimental

Materials

Inosine (Ino), guanosine (Guo), N(7)-methylguanosine (m^7Guo), 2-[N-morpholino]ethanesulfonic acid (Mes), N-2-hydroxyethylpiperazine-N′-2-ethanesulfonic acid (Hepes, Sigma Ultra grade), mono- and dibasic sodium phosphates (P_i), KCl (ACS grade), and xanthine oxidase from buttermilk (grade III, 1 U/mg) were products of Sigma Chemical Co. (St. Louis, MO, USA). Sodium acetate was from POCh (Gliwice, Poland), acetic acid and sodium hydroxide from Merck (Darmstadt, Germany). Sodium thiophosphate (SP_i, tribasic, dodecahydrate), from Aldrich (USA), with reported purity >97%, was found to contain a background amount (~1.2%) of P_i, as determined by ^{31}P NMR (data not shown), and see, below, section on SP_i (inorganic thiophosphate) as cosubstrate.

The PNP from human erythrocytes (lyophilized powder) was a product of Sigma. Partially purified PNP-I from *E. coli* (~60% pure, about 60 U/mg), a gift of Dr. G. Koszalka (Wellcome Research Labs, Research Triangle Park, NC, USA), was further purified to apparent homogeneity according to Kierdaszuk et al. (1997).

Buffered solutions, selected to avoid buffer effects on enzyme activity, previously noted with Tris and other buffers (Stoychev et al. 2001), were prepared with sodium acetate (pH 4.5–5.5), Mes (pH 6) and Hepes (pH 7–8) using high-quality MilliQ water, and appropriate pH adjusted with acetic acid (pH 4.5–5.5) and NaOH (pH 6–8). Solutions contained background contaminant phosphate, ≤1 μM, determined spectrophotometrically (Ames 1966), and taken into account during preparation of solutions containing different concentrations of P_i.

Concentrations of substrates were determined spectrophotometrically from their molar extinction coefficients: at pH 7.0 for Ino, ε(249 nm) = 12,300 M^{-1} cm^{-1} and Guo, ε(253 nm) = 13,700 (Dawson et al. 1969); at pH 2.0 for m^7Guo, ε(257 nm) = 10,900 (Hendler et al. 1970). Protein concentration was measured spectrophotometrically at pH 7.0 from their extinction coefficients: $\varepsilon^{1\%}_{278} = 2.7$ for PNP-I (Bzowska et al. 1998) and $\varepsilon^{1\%}_{280} = 9.64$ for human PNP (Stoeckler et al. 1978a).

Enzyme assays

Enzyme activity was monitored spectrophotometrically at 25°C in 50 mM appropriate buffer (see section on Materials), by the coupled xanthine oxidase procedure with Ino as substrate (Stoeckler et al. 1978b), and/or more directly with Guo or m^7Guo by following the changes in absorption at 260 nm. Values of $\Delta\varepsilon$ ($\times 10^{-3}$) between substrate (Guo or m^7Guo) and product (Gua or m^7Gua) at 260 nm were as follows: 4.5 for Guo (pH 5–8), and 6.5 (pH 5.0–5.5), 6.0 (pH 6, Stoychev et al. 2001), 3.8 (pH 7) and 2.0 (pH 8) for m^7Guo.

UV absorption was monitored with a Kontron (Switzerland) Uvikon 930 spectrophotometer equipped with a thermostatically controlled cell compartment, using 2-, 5- or 10-mm pathlength cuvettes. Measurements of pH (±0.05) were done with a Jenway (UK) pH-meter equipped with a combination semi-micro electrode and temperature sensor.

Phosphorolysis was followed in a reaction mixture of 300 to 1,200 µl containing a nucleoside (Ino, Guo or m^7Guo), P_i or SP_i, and PNP at appropriate concentrations. For kinetic measurements with P_i, with Ino as substrate, the xanthine oxidase employed was filtered through Centricon 30 in 50 mM Hepes/NaOH pH 7.0 with 1 mM EDTA and 1 mM sodium salicylate, to remove ammonium sulphate, a known inhibitor of PNP-I (Kierdaszuk et al. 1997). PNP concentration was adjusted to give a linear, 2- to 5-min, initial reaction progress, and a linear dependence of the reaction rate on enzyme concentration. The enzyme was stored at pH 7 and added 10 min before an experiment to the reaction mixture containing the nucleoside substrate at the desired pH. Addition of the second substrate (P_i or SP_i) initiated the reaction. Both enzymes were stable during the course of phosphorolysis at acidic pH (<6); incubation for 10 min at low pH was without effect on activity, and >90% activity was retained after 30 min incubation.

Kinetic parameters for P_i and SP_i were determined in the presence of a nucleoside concentration, at least fivefold higher than its K_m at a given pH. This gave at least 83% of maximum rate, and was particularly important in the case of m^7Guo, which consists of an equilibrium mixture of the cationic and the zwitterionic forms (pK_a 7) with comparable activities with PNP-I (Stoychev et al. 2001), as well as with the human enzyme (data not shown).

The m^7Guo was selected as a convenient nucleoside substrate, because its phosphorolysis is easily followed by the marked differences between absorption spectra of m^7Guo and m^7Gua (product) at pH 5–8. In contrast, spectrophotometric assay of phosphorolysis of Guo (at saturated concentration) was complicated by the strong inhibition detected for the product Gua (data not shown). In the case of phosphorolysis of Ino, applicability of the coupled xanthine oxidase assay at pH <6 was precluded by the low activity of xanthine oxidase at this pH, and its instability following removal of the ammonium sulphate (a PNP inhibitor) by filtration on Centricon 30.

The specific activities of the enzymes were determined at 25°C with 0.5 mM Ino and 50 mM phosphate buffer (pH 7) by the coupled xanthine oxidase procedure. The formation of product was determined from the changes in absorption between Ino and the final product of the coupled reaction (uric acid) at 300 nm, for which $\Delta\varepsilon$ = 9,600 M^{-1} cm^{-1}. One unit of PNP activity is defined as 1 µmol Ino phosphorolysed per minute under these conditions. The enzymes from *E. coli* and human erythrocytes had specific activities of 87 and 28 U mg^{-1}, respectively.

Enzyme kinetics

Kinetic constants were determined using the initial rate method. Initial rates (v_o) were determined from linear regression fitting to at least 10 experimental points with a relative error of ≤5%. Kinetic constants were obtained from non-linear regression analysis (see below). Fitting to 10–20 initial rates covered the whole concentration range of the substrate ([S]). The reduced chi-square (χ^2_R) values and residuals between experimental (v_o^{exp}) and theoretical (v_o^{teo}) values normalized to the calculated error, i.e. $(v_o^{exp} - v_o^{teo})/\sqrt{v_o^{exp}}$, were used to test the quality of the fits.

Values of the Michaelis constant (K_m) and maximal velocity (V_{max}) were obtained from fitting of the Michaelis–Menten equation (Eq. 1):

$$v_o = \frac{V_{max}[S]}{[S] + K_m} \quad (1)$$

In case of a poor fit of Eq. 1, fitting was performed with the Adair equation (Eq. 2) (Neet 1980) within the sequential model based on the theory of Koshland et al. (1966), which takes into account cooperativity of two binding sites:

$$v_o = \frac{2V_{max\,1}K_{m2}[S] + 2V_{max\,2}[S]^2}{K_{m1}K_{m2} + 2K_{m2}[S] + [S]^2} \quad (2)$$

where V_{max1} and V_{max2} are the maximal velocities of decomposition of the enzyme/nucleoside/P_i complexes with one and two sites occupied by P_i into free enzyme and products, K_{m1} and K_{m2} are the observed apparent Michaelis constants, which are equal to the microscopic P_i dissociation constants of the particular complexes, assuming rapid establishment of equilibrium between substrates and the substrate–enzyme complex, and slow decomposition of the complex into free enzyme and products. The relations between the two Michaelis constants, $K_{m1} < K_{m2}$ and

$K_{m1} > K_{m2}$, are characteristic of negative and positive cooperativity of substrate binding, respectively.

To visualize graphically deviations from hyperbolic dependence of initial rates on substrate concentration (Eq. 1), the Eadie–Hofstee form (Eq. 3) of the Michaelis–Menten equation was applied.

$$v_o = V_{max} - K_m v_o/[S] \quad (3)$$

Cooperativity of enzyme kinetics was also analysed according to the Hill equation (Eq. 4). The Hill coefficient (n_H) was used as a measure of cooperativity, i.e. negative cooperativity ($n_H < 1$) and positive cooperativity ($n_H > 1$), as follows:

$$v_o = \frac{V^H_{max}[S]^{n_H}}{[S]^{n_H} + (K^H_m)^{n_H}} \quad (4)$$

or in the linear form

$$\log \frac{v_o}{V^H_{max} - v_o} = n_H \log [S] - n_H \log K^H_m \quad (5)$$

where K^H_m and V^H_{max} are the apparent Michaelis constant and maximal velocity, respectively.

Results

The heterogeneous affinity of PNP-I for P_i at pH 7.6 (Kierdaszuk et al. 1997), and its putative dependence on the ionic form of the phosphate, prompted us to determine the kinetic parameters, K_m and V_{max}, for phosphorolysis of m^7Guo by PNP-I with its natural cosubstrate, P_i, as well as with its close structural analogue, thiophosphate (SP_i). The latter was initially observed to compete weakly with P_i, indicating that SP_i is bound, albeit poorly. Reactions were run in the pH range 5–8, where P_i and SP_i are equilibrium mixture of mono- and dianionic forms, pK_a = 6.7 and 5.4, respectively (Gerlt et al. 1982; Jaffe and Cohn 1978; Jungas 2006, and references cited). Analogous kinetic measurements were performed with human PNP, which is active only against 6-oxopurine nucleosides.

The observed kinetics for both enzymes with P_i are non-Michaelis, and better described by the sequential model (Eq. 2), for a system with cooperative binding of substrates (Table 1). The one exception is the kinetics of human PNP at pH 5.0 and 5.3 (see next section).

pH-dependence of kinetic parameters for P_i

Increase of pH from 5 to 8 leads to better substrate properties of P_i for both enzymes (Fig. 2), described by two sets of kinetic parameters for PNP-I (pH 5–8) and the human enzyme (pH 6–8) (Table 1). One of the two sets of parameters showed poorer catalytic properties at each pH (higher K_m and lower value of V_{max}/K_m), pointing to factors common to both.

With PNP-I, the V_{max1}/K_{m1} (Fig. 2) derived from the sequential model (Eq. 2) increases 21-fold, from 0.01 at pH 5 to 0.21 l mg^{-1} min^{-1}at pH 6, mainly due to an increase of V_{max1} (Table 1). Further increase of pH to 7, and subsequently to 8, led to fivefold and tenfold increases of V_{max1}/K_{m1}, respectively, largely due to a gradually decreasing K_{m1}. Concomitantly, V_{max2}/K_{m2} increases with an increase in pH from 5 to 8. The 12-fold increase of V_{max2}/K_{m2}, from 0.0055 at pH 5 to 0.066 l $mg^{-1}min^{-1}$ at pH 6, resulted from

Table 1 The pH-dependence of the Hill coefficient (n_H), and apparent Michaelis constants (K_{m1}, K_{m2}) and apparent maximal velocities (V_{m1}, V_{m2}) of P_i for phosphorolysis of m^7Guo (at saturated concentration) by PNP from *E. coli* (PNP-I) and human erythrocytes, from non-linear least-squares fittings ($\chi^2_R \sim 1$) of the Hill model (Eq. 4) and sequential model (Eq. 2), respectively

pH	n_H	K_{m1} [μM]	V_{max1} [μmol min^{-1} mg^{-1}]	V_{max1}/K_{m1} [L min^{-1} mg^{-1}]	K_{m2} [μM]	V_{max2} [μmol min^{-1} mg^{-1}]	V_{max2}/K_{m2} [L min^{-1} mg^{-1}]
E. coli PNP-I							
5.0	0.93 ± 0.01	37 ± 8	0.35 ± 0.05	0.010	508 ± 15	2.8 ± 0.1	0.0055
5.3	0.83 ± 0.01	46 ± 3	2.9 ± 0.1	0.063	200 ± 6	6.1 ± 0.1	0.031
6.0	0.74 ± 0.04	33 ± 3	7 ± 2	0.21	123 ± 10	8.1 ± 0.2	0.066
7.0	0.63 ± 0.07	15 ± 2	16 ± 1	1.1	135 ± 45	11 ± 1	0.083
8.0	0.70 ± 0.04	0.6 ± 0.3	6 ± 1	10	15 ± 3	12 ± 1	0.83
Human PNP							
5.0[a]	1.01 ± 0.05	1152 ± 67	4.9 ± 0.1	0.0043	–	–	–
5.3[a]	1.01 ± 0.04	419 ± 20	10 ± 1	0.024	–	–	–
6.0	0.71 ± 0.03	92 ± 19	9 ± 2	0.10	384 ± 23	8.9 ± 0.4	0.023
7.0	0.58 ± 0.03	5 ± 2	16 ± 2	3.2	58 ± 14	16 ± 1	0.28
8.0	0.50 ± 0.04	1.3 ± 0.4	16 ± 2	12	34 ± 9	22 ± 1	0.64

[a] Enzyme kinetics described by the Michaelis–Menten model (Eq. 1) with a single set of kinetic parameters, and Hill model with $n_H \sim 1$

both an increase of V_{max2} and decrease of K_{m2}. In the pH range from 6 to 7 the increase of V_{max2}/K_{m2} was small, but further elevation of pH to 8 led to a tenfold increase, due to a marked decrease of K_{m2}. Thus, the increase of pH from 5 to 8 resulted in substantial increases of V_{max1}/K_{m1} and V_{max2}/K_{m2} (Fig. 2, Table 1), three and two orders of magnitude, respectively.

With the human enzyme a single set of kinetic parameters (V_{max} and K_m) was found in the pH range 5.0–5.3 (Eq. 1), with a >5-fold increase of V_{max}/K_m at pH 5.3 relative to that at pH 5.0, due to an increase of V_{max} and a concomitant decrease of K_m (Fig. 2, Table 1). At pH > 5.3 the kinetics for P_i is described by two sets of parameters; both V_{max1}/K_{m1} and V_{max2}/K_{m2} increase monotonically with pH, leading to 120- and 25-fold increases, respectively, at pH 8. As for the bacterial enzyme, the V_{max1}/K_{m1} values are at least fivefold higher than the corresponding V_{max2}/K_{m2}, and the differences were accentuated at higher pH (Fig. 2).

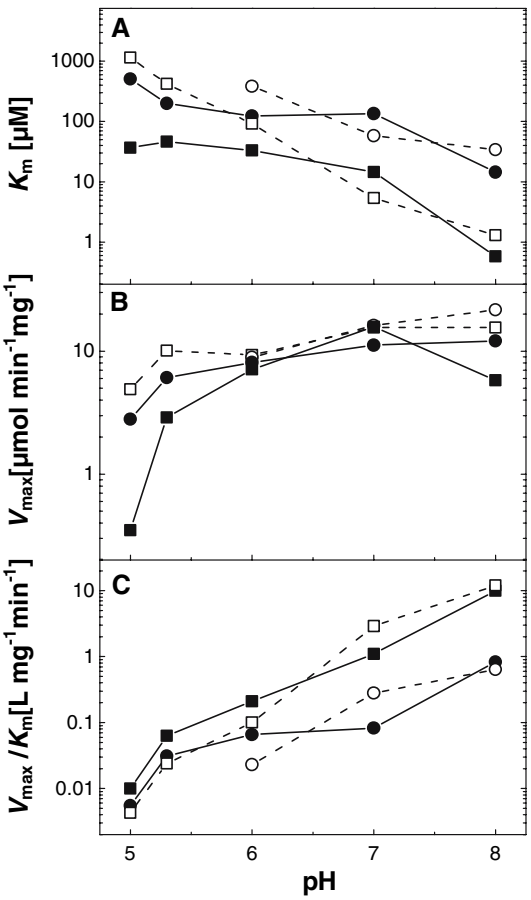

Fig. 2 The pH-dependence of the kinetic parameters K_m (upper frame), V_{max} (middle frame) and V_{max}/K_m (bottom frame) of P_i for phosphorolysis of m^7Guo (at saturated concentration) by PNP from human erythrocytes (*dashed line*) and *E. coli* (*solid line*). Note two sets of kinetic parameters (A) K_{m1} (*dashed line with open squre* or *solid line with filled square*) and K_{m2} (*dashed line with open circle* or *solid line with filled circle*); (B) V_{max1} (*dashed line with open squre* or *solid line with filled square*) and V_{max2} (*dashed line with open circle* or *solid line with filled circle*); (C) V_{max1}/K_{m1} (*dashed line with open squre* or *solid line with filled square*) and V_{max2}/K_{m2} (*dashed line with open circle* or *solid line with filled circle*) resulted from nonlinear least-squares fittings of the sequential model (Eq. 2). Reasonable good fits of the simpler Michaelis-Menten model (Eq. 1) were obtained for the human enzyme at pH 5.0 and 5.3, only. Estimated standard deviations are not higher than 20% for K_{m1}, K_{m2} , V_{max1}/K_{m1} and V_{max2}/K_{m2}; 15% for $V_{max1,}$ and 5% for V_{max2}

Analysis of the crystal structures of PNPs, homotrimeric from mammals (Ealick et al. 1990; Koellner et al. 1997; Narayana et al. 1997; Mao et al. 1998), and homohexameric from *E. coli* (Mao et al. 1997) and *Plasmodium falciparum* (Schnick et al. 2005), revealed the same tertiary fold in each enzyme subunit in a given structure, especially around the substrate binding sites. Therefore, the non-Michaelis kinetics likely derive from interactions between active sites upon binding of substrates, and not the mere presence of several independent binding sites.

Eadie-Hofstee plots as a function of pH are shown in Fig. 3. The experimental data points depart from linearity in a manner characteristic of negative cooperativity, except for phosphorolysis by human PNP at pH 5.0 to 5.3. This is supported by fitting of the Hill equation (Eq. 4), with a Hill coefficient (n_H) less than unity for the bacterial and human enzymes in the pH ranges from 5 to 8, and 6 to 8, respectively (Table 1).

The cooperativity described above is in line with that previously observed for binding of P_i to PNP-I at pH 7.6 (Kierdaszuk et al. 1997), as well as for phosphorolysis of Ino at pH 7 (Fig. 4). In the latter case, enzyme kinetics for P_i is described by a Hill coefficient 0.56 ± 0.02 (Fig. 4, inset), and two sets of K_m and V_{max} values, 133 ± 20 μM and 44 ± 3 μmol min^{-1}mg^{-1}, and 1.7 ± 0.3 mM and 45 ± 1 μmol min^{-1}mg^{-1}, derived from the sequential model (Eq. 2). Previous kinetic measurements of Ino phosphorolysis by PNP-I at pH 7.1 (Jensen and Nygaard 1975), and by human PNP at pH 7.5 (Choi et al. 1986) also showed cooperativity with respect to P_i, i.e. a non-linear dependence of $1/v_o$ versus $1/[P_i]$. In line with the foregoing, negative cooperativity was also observed with P_i for phosphorolysis of Guo by PNP-I (n_H = 0.68 ± 0.01 and 0.76 ± 0.02 at pH 5.0 and 8.0, respectively), and by the human enzyme (n_H = 0.69 ± 0.05 at pH 8) (data not shown).

SP_i (inorganic thiophosphate) as cosubstrate

The thiophosphate analogue of P_i, SP_i, has a pK_a of 5.4, hence well below that of P_i (pK_a 6.7) and, at pH >6, exists predominantly as the dianion. In initial experiments it was found that SP_i competes weakly with P_i, subsequently shown to be due to its ability to replace P_i as a weak cosubstrate.

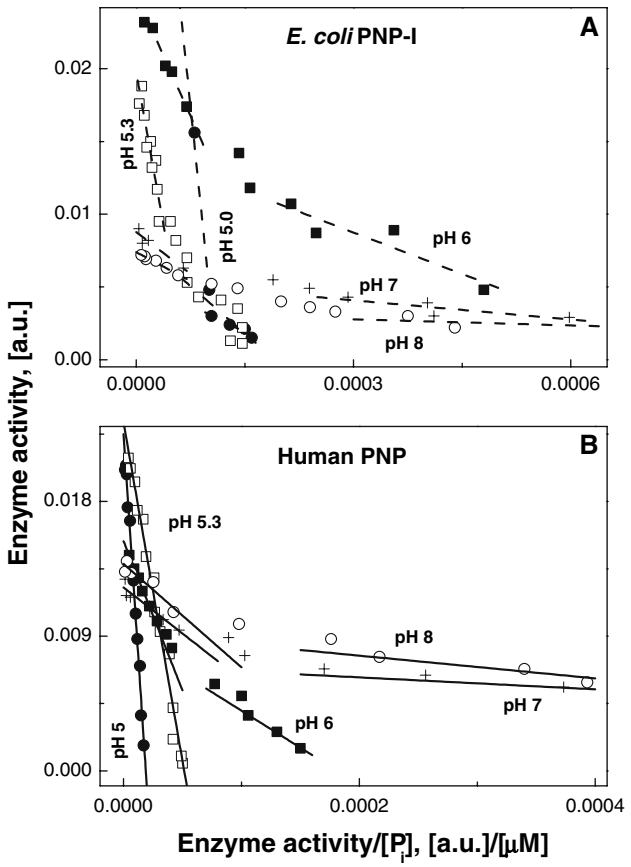

Fig. 3 Eadie-Hofstee plots (Eq. 3) against P_i concentration for phosphorolysis of m^7Guo (at saturated concentration) catalysed by PNP from *E. coli* (PNP-I) (A) and human erythrocytes (B) at pH 5.0 (*filled circle*), 5.3 (*open square*), 6.0 (*filled square*), 7.0 (*plus*) and 8.0 (*open circle*). Note two sets of linear plots (A) pH 5.0 (*dashed line with filled circle with dashed line*), pH 5.3 (*dashed line with open square with dashed line*), pH 6.0 (*dashed line with filled square with dashed line*), pH 7.0 (*dashed line with plus with dashed line*) and pH 8 (*dashed line with open circle with dashed line*); (B) pH 6.0 (*solid line with filled square with solid line*), pH 7.0 (*dashed line with plus with dashed line*) and pH 8.0 (*dashed line with open circle with dashed line*) resulted from least-squares fittings of Eq. 3 to linear portions of the experimental data

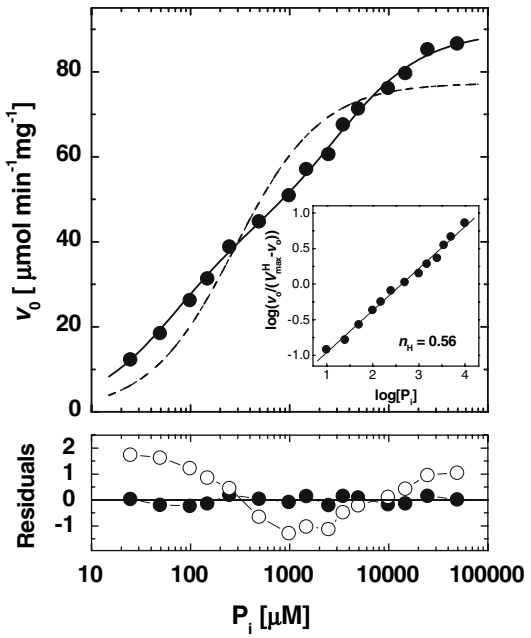

Fig. 4 Comparison of the theoretical values of the best fits of the Michaelis-Menten model (Eq. 1) (*dashed line*) and the sequential model (Eq. 2) (*solid line*) to dependence of initial rates (v_o) against P_i concentration for phosphorolysis of 5 mM Ino catalysed by PNP from *E. coli* in 50 mM Hepes pH 7. The lower panel shows the residual differences between experimental (v_o^{exp}) and theoretical (v_o^{teo}) values normalized to errors, i.e. $(v_o^{exp} - v_o^{teo})/\sqrt{v_o^{exp}}$, and shown by open (Eq. 1) and filled (Eq. 2) circles. Inset shows a Hill plot of the same data, and results of fitting of the linear form of the Hill equation (Eq. 5)

However, monitoring SP_i kinetics posed some difficulties, due to its contamination with ~1.2% P_i (see Materials). To minimize background phosphorolysis by contaminant P_i to a level at least an order of magnitude lower than that with SP_i, kinetic measurements were performed with SP_i concentrations such that the concentration of contaminant P_i was at least sixfold lower than its K_m (or K_{m1}) at a given pH. Nonetheless, it was not possible to determine kinetic parameters with SP_i for both enzymes at pH 8 (where K_m ~1 μM for P_i), or with human PNP at pH 5 (where activity vs SP_i is barely detectable).

Phosphorolysis of Ino or m^7Guo at pH from 5 to 8 was not detectable prior to addition of SP_i. Kinetics with both PNPs are properly described by the simple Michaelis–Menten model (Eq. 1). Kinetic constants, K_m and V_{max}/K_m, exhibited only very weak pH-dependence for both enzymes (Table 2), consistent with the fact that, at pH >6, SP_i exists predominantly as the dianion. In contrast, the results for P_i clearly show that the marked enhancement of P_i substrate properties on elevation of pH from 5 to 8 correlates with the increasing proportion of its dianionic form, from 2 to 95%. This implies that, for both enzymes, the P_i dianion is a much better substrate than its monoanion. Furthermore, elevation of the level of the P_i dianion leads to higher cooperativity, i.e. the V_{max1}/K_{m1} to V_{max2}/K_{m2} ratio increases, whereas the Hill coefficient (n_H) decreases, with increase of pH (Fig. 2, Table 1).

The ability of SP_i to replace P_i in the phosphorolytic pathway, albeit weakly, requires consideration of possible interference by phosphorolysis with contaminant P_i in the buffer media (≤1 μM) and in the SP_i employed (~1%) (see Materials and this section), and, furthermore, the hydrolytic reaction, in the absence of phosphate, reported for Ino and Guo (Kline and Schramm 1992, 1995) and m^7Guo (Bzowska 2002) with calf spleen PNP. Hydrolysis of Ino by calf spleen PNP in the absence of phosphate has also been observed in the crystal structure of their complex (Mao et al. 1998).

Table 2 The pH-dependence of the kinetic parameters (K_m, V_{max} and K_m/V_{max}) of SP_i for phosphorolysis of m^7Guo (at saturated concentration) by PNP from *E. coli* (PNP-I) and human erythrocytes, from non-linear least-squares fittings ($\chi^2_R \sim 1$) of the Michaelis-Menten model (Eq. 1)

pH	K_m [μM]	V_{max} [μmol min^{-1} mg^{-1}]	V_{max}/K_m [L mg^{-1} min^{-1}]
E. coli PNP-I			
5.0	69 ± 7	0.53 ± 0.05	0.0077 ± 0.0011
6.0	97 ± 26	4.5 ± 0.6	0.046 ± 0.014
7.0	87 ± 19	3.3 ± 0.3	0.038 ± 0.009
Human PNP			
6.0	74 ± 16	3.8 ± 0.3	0.051 ± 0.012
7.0	40 ± 8	10.7 ± 1.0	0.27 ± 0.06

In order to evaluate the effect of background phosphorolysis in our experiments with contaminant P_i in SP_i samples, a comparison was made between experiments performed with (1) SP_i plus contaminant P_i, and (2) with P_i at the same concentration as that of contaminant P_i (data not shown). This demonstrated that background phosphorolysis with contaminant P_i was at least an order of magnitude lower than that with SP_i, and that of contaminant P_i in the buffer media at least two orders of magnitude lower. Under these conditions, we observed no detectable activity on prolonged incubation of both PNPs with nucleoside substrates when no extra P_i or SP_i was added. Furthermore, possible hydrolysis of SP_i to P_i during prolonged incubation can also be excluded, because this would have led to detectable phosphorolysis.

Finally, and most important, it should be noted that the concentrations of enzyme required to detect enzymatic hydrolysis of Ino and Guo (1 μM) and m^7Guo (5 μM) were at least 10^3-fold higher than those employed here. For hydrolysis of Ino in the crystal structure, it was even much higher.

It remains to add that PNP-II, the specificity of which differs from that of PNP-I (see Introduction), was also found to accept SP_i as a weak cosubstrate (data not shown).

Discussion

The role of the ionic forms of P_i in the mechanism of phosphorolysis by PNP is relevant to the assumed stabilizing role of the dianion in the transition-state oxocarbenium complex in the model proposed for phosphorolysis by human PNP (Erion et al. 1997b; Lewandowicz and Schramm 2004), and considered to apply to other PNPs (Pugmire and Ealick 2002).

Although our results do not exclude substrate activity of the monoanion of P_i, the pH-dependence of V_{max}/K_m strongly suggests that the dianion is the better substrate, by three orders of magnitude. This is in line with previously reported observation that P_i binds to human PNP as the dianion (Deng et al. 2006). We are unable to exclude initial binding of the monoanion, followed by dissociation to the dianion. Such a possibility is indicated by studies with the aid of NMR (Sauve et al. 2003) and vibrational (Deng et al. 2004) spectroscopy. The phosphate binding sites containing three Arg residues in PNP-I (Mao et al. 1997; Koellner et al. 1998), and two Arg residues and one His in the human enzyme (Ealick et al. 1990), are able to accommodate both the monoanion and the dianion of P_i.

Decrease of substrate activity of P_i at pH ~5 may also result from protonation of amino acid residues in the active site. With human PNP, the most important are His86 and Glu89 in the phosphate-binding site, His257 in the ribose-binding site, and Glu201 in the base-binding site. With PNP-I, protonation may occur on His4 in the ribose-binding site, and Asp204 in the base-binding site (see further below).

Kinetics of phosphorolysis by both enzymes with P_i are non-Michaelis, and exhibit negative cooperativity described by a model of two enzyme states with low and high affinity towards P_i. These "states" of the enzyme are defined as enzyme-substrate complexes with one or two active sites occupied by P_i, characterized by low and high values of the microscopic dissociation constants (apparent Michaelis constants, $K_{m1} < K_{m2}$), respectively. Formation of the high-affinity enzyme–ligand complex by association of P_i to one active site of a homotrimeric PNP (human PNP), or one site in each dimer of a tri-dimeric (homohexameric) PNP (PNP-I) would lead to an enzyme state with low affinity for the second P_i cosubstrate. This is in accord with results of earlier studies on P_i binding by PNP-I at pH 7.6 (Kierdaszuk et al. 1997). The "high-affinity state" would then exist at a P_i concentration range of several tens of μM ($K_d \sim 30$ μM). Further increase of P_i concentration then converts the enzyme to a "low-affinity state" ($K_d \sim 1$ mM), which may account for the fact that enzyme kinetics at high concentrations of P_i is characterized by higher K_m and lower V_{max}/K_m values.

An obvious candidate for the high-affinity state is the enzyme free of ligand. Formation of the low-affinity state requires transmission of the effect of P_i binding via electrostatic interactions and/or conformational transitions towards a neighbouring active site. It is of interest, in this context, that the solid-state structures of the hexameric PNP-I (Koellner et al. 1998, 2002) show that it may be a trimer of one symmetrical and two unsymmetrical dimers (Koellner et al. 1998), as well as a trimer of unsymmetrical dimers containing pairs of monomers with active sites in different conformations induced by binding of different ligands (Koellner et al. 2002), i.e. phosphate (sulphate) and

m^6FA, and phosphate (sulphate) and m^7FA, respectively. In addition, interaction with P_i in one active site of the dimer may result in structural changes leading to a lower affinity of the second site, because each phosphate binding site contains an Arg43 residue from a neighbouring subunit.

Interaction of the inhibitor m^6FA with PNP-I (Kierdaszuk et al. 2000) is a striking example of the effect of P_i on PNP-I affinity and specificity versus inhibitors. This inhibitor exhibits an amino-imino tautomeric equilibrium in aqueous solution. The imino tautomer of m^6FA was found to be bound selectively by the enzyme in the absence of P_i; by contrast, addition of P_i shifted the binding to the amino species with a dissociation constant K_d ~0.5 μM, two orders of magnitude lower than that in the absence of P_i (K_d ~46 μM). As pointed out earlier (see Introduction), this is a good illustration of the complementary utility of solution and solid state methods, inasmuch as the crystal structures of PNP-I with FB and P_i (Koellner et al. 1998), and m^6FA, m^7FA and P_i (Koellner et al. 2002) were unable to resolve the tautomeric form of the bound formycin ligand.

With trimeric PNPs, the crystal structure of calf PNP (Mao et al. 1998) showed that P_i binding led to marked conformational transitions in the phosphate binding site by movements of the loops of residues 33–36 and 56–69, also dependent on the degree of saturation of the phosphate binding sites by P_i, and pointing to involvement of communication between subunits. The latter may be mediated by Phe159 from a neighbouring subunit, engaged in the ribose-binding site.

It is worthy of note that, for both enzymes, the catalytic efficiency of "the high-affinity state" (V_{max1}/K_{m1}) increases much more than that of "the low-affinity state" (V_{max2}/K_{m2}) as the pH increases from 5 to 8. Thus, a correlation exists between the population of the P_i dianion and the magnitude of cooperativity, reflected by a decrease in the Hill coefficient to ~0.5 at pH 8 (Table 1). For the same reason, cooperativity is absent at pH 5 and 5.3, where P_i exists predominantly as the monoanion, and typical Michaelis kinetics is observed with human PNP.

In the case of PNP-I, an increase in the Hill coefficient (decrease of cooperativity) with decrease in the pH (Table 1) could be caused by electrostatic interaction between P_i and Arg24, reflected by structural differences around Arg24 of the unsymmetrical active sites of each dimer (Koellner et al. 2002). Moreover, Bennett et al. (2003), who determined the three-dimensional structure of the enzyme complexed with various nucleoside analogues, reported that Arg24 is in close contact with the phosphate ligand only in one of the three independent active sites, and is quite distal (up to 8 Å) from the other two. Thus, location of Arg24 in the active sites may affect binding of P_i and, due to the positive charge on Arg, its electrostatic interaction with P_i would be dependent on the monoanion–dianion equilibrium of P_i, hence also on pH.

The magnitude of the cooperative effect may also be affected by protonation of His4 in the ribose-binding site of PNP-I. His4 belongs to a neighbouring subunit and forms a hydrogen bond with the oxygen of the ribose 5′-OH of the nucleoside substrate. With mammalian PNPs it has been proposed that the 5′-OH is essential in formation and stabilization of the transition state, and appropriate rearrangement of this group is achieved by interaction with His257 (Kicska et al. 2002), the location of which, relative to ribose, is similar to that of His4 in the bacterial enzyme. It is conceivable that the same stabilizing interaction occurs in PNP-I, but there is a major difference between the two enzymes, in that His4 comes from a neighbouring subunit, but His257 does not.

The lack of cooperativity for human PNP at pH ~5 (Table 1) can be explained by protonation of His86 or Glu89 in the phosphate-binding site. These two residues are predicted to be catalytically important, based on their interaction with P_i in the crystal structure, the 10- to 25-fold reduction of catalytic activity observed for the His86Ala and Glu89Ala mutants (Erion et al. 1997a,b), and the total lack of activity of a natural mutant, Glu89Lys, isolated from PNP-deficient patients (Williams et al. 1987).

It is worth noting that negative cooperativity with P_i occurs not only for phosphorolysis of m^7Guo and Ino, but also for Guo at pH 8 with both enzymes, and at pH 5 with PNP-I. The observed cooperative effects of P_i accompanying phosphorolysis of natural nucleosides indicate that P_i plays a key role in their catabolism by regulation of the intracellular activity of the enzyme.

In accord with the foregoing, we would like to recall studies of the effect of the concentration of P_i on the affinity of the enzyme for bisubstrate analogue inhibitors, including acyclovir diphosphate (Tuttle and Krenitsky 1984), nucleotide analogue inhibitors (Krenitsky et al. 1990) and antiviral acyclic nucleoside phosphonates (Kulikowska et al. 1998). Remarkably, such inhibitors are more effective at the low mM P_i concentration prevailing in human cells (Traut 1994), conferring added confidence to the important role of negative cooperativity. Other examples are mentioned above, e.g. an influence of phosphate on the affinity of FA and its methylated analogues (m^6FA, m^7FA) to *E. coli* PNP-I (Kierdaszuk et al. 2000; Koellner et al. 2002).

The ability of PNP to accommodate inorganic thiophosphate, in place of P_i, as a cosubstrate, albeit a weak one, is of considerable interest, bearing in mind the larger van der Waals radius of sulfur (1.85 Å vs 1.40 Å), and the longer P–S (1.94 Å) bond relative to P–O (1.57 Å). In addition to these steric differences between a thiophosphoryl group and

a phosphoryl group, there is a distinct difference in charge distribution in the respective anions. It is now well established that, in both the SP_i monoanion and dianion, one negative charge is localized on the sulfur atom, whereas the second charge in the dianion is delocalized between two oxygen atoms (Frey and Sammons 1985; Frey 1989). There is, consequently, an unequal distribution of charge amongst the three non-bridging atoms of the thiophosphoryl group as compared to the P_i dianion (Fig. 5). Furthermore, localization of a negative charge on sulfur (which is more stable than a negative charge localized on oxygen) in both anions of thiophosphate is consistent with the stronger acidities of these species (Frey and Sammons 1985), the pK_a values for which are 1.67, 5.40 and 10.14, as compared to 2.1, 6.7 and 12.3 for the corresponding phosphates.

Distances between the oxygen atoms of P_i (sulphate) and adjacent amino acids in the crystallographic structures of PNPs from *E. coli* (1K9S.pdb, Koellner et al. 2002; 1A69.pdb, Koellner et al. 1998) and human erythrocytes (1RCT.pdb, Canduri et al. 2004; 1PF7.pdb, de Azevedo et al. 2003) suggest that the P_i binding site should readily accommodate the slightly larger SP_i anion.

In light of the foregoing, it is of interest that the 5′-phosphorothioate of adenosine, ATPγS, is a >200-fold better inhibitor of a protein tyrosine phosphatase than ATP; furthermore, although P_i is a very weak inhibitor, SP_i is 30-fold more effective (Zhao 1996). SP_i is also a better inhibitor of 5′-nucleotidase from rat liver membrane than is P_i (Naito and Lowenstein 1985). SP_i was long ago reported to be a slightly more effective inhibitor than P_i of O-phosphorothioate hydrolysis by *E. coli* alkaline phosphatase (Chlebowski and Coleman 1974). These findings would have been more informative if they had been conducted at several pH values; e.g. the pH-dependence of the time-dependent inhibition of thymidylate synthase by 5-fluoro-dUMP and its 5′-thiophosphate analogue, 5-fluoro-dUMPS, was found to correlate with the difference in pK_a values of the phosphate and thiophosphate groups, pointing to a preference in the active centre of the enzyme for the dianionic phosphate group (Golos et al. 2001).

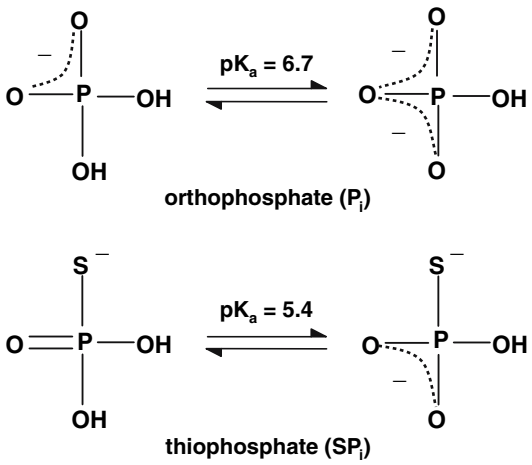

Fig. 5 The mono- and dianionic forms of orthophosphate (P_i) and thiophosphate (SP_i)

Acknowledgment We are indebted to Prof. Ryszard Stolarski (Department of Biophysics, University of Warsaw) for critical reading of the manuscript. This investigation was supported by the Polish Ministry of Scientific Research and Higher Education (MNSzW), grant No. 3P04A02425.

References

Ames BN (1966) Assay of inorganic phosphate. Methods Enzymol 8:115–116

Behlke J, Koellner G, Bzowska A (2005) Oligomeric structure of mammalian purine nucleoside phosphorylase in solution determined by analytical ultracentrifugation. Z Naturforsch 60C:927–931

Bennett EM, Li C, Allan PW, Parker WB, Ealick SE (2003) Structural basis for substrate specificity of *Escherichia coli* purine nucleoside phosphorylase. J Biol Chem 278:47110–47118

Bzowska A, Kazimierczuk Z, Seela F (1998) 7-Deazapurine 2′-deoxyribofuranosides are noncleavable competitive inhibitors of *Escherichia coli* purine nucleoside phosphorylase (PNP). Acta Biochim Polon 45:755–768

Bzowska A, Kulikowska E, Shugar D (2000) Purine nucleoside phosphorylases: properties, functions, and clinical aspects. Pharmacol Ther 88:349–425

Bzowska A (2002) Calf spleen purine nucleoside phosphorylase: complex kinetic mechanism, hydrolysis of 7-methylguanosine, and oligomeric state in solution. Biochim Biophys Acta 1596:293–317

Bzowska M, Stępniak K, Olasek M, Długosz M, Wielgus-Kutrowska B, Antosiewicz J, Holy A, Koellner G, Stroh A, Raszewski G, Steiner T, Frank J (2005) Attempts to differentiate subunits of trimeric and hexameric purine nucleoside phosphorylases by crystal structure and solution studies using purine bases, modified purine nucleosides, acyclonucleosides and their phosphonate analogues. Collection Czechoslov Chem Commun 7:133–142

Canduri F, dos Santos DM, Silva RG, Mendes MA, Basso LA, Palma MS, de Axevedo WF, Santos DS (2004) Structures of human purine nucleoside phosphorylase complexed with inosine and ddI. Biochem Biophys Res Commun 313:907–914

Chlebowski JF, Coleman JE (1974) Mechanisms of hydrolysis of O-phosphorothioates and inorganic thiophosphate by *Escherichia coli* alkaline phosphatase. J Biol Chem 249:7192–7202

Choi H-S, Stoeckler JD, Parks RE Jr (1986) 5-Iodoribose 1-phosphate, an analog of ribose 1-phosphate. Enzymatic synthesis and kinetic studies with enzymes of purine, pyrimidine, and sugar phosphate metabolism. J Biol Chem 261:599–607

Dawson RMC, Elliott DC, Elliott WH, Jones KM (eds) (1969) Spectral data and pK values for purines, pyrimidines, nucleosides and nucleotides. In: Data for biochemical research. Oxford University Press, Oxford, p 176

Dandanell G, Szczepanowski R, Kierdaszuk B, Shugar D, Bochtler M (2005) *Escherichia coli* purine nucleoside phosphorylase II, the product of the *xapA* gene. J Mol Biol 348:113–125

de Azevedo WF Jr, Canduri F, Dos Santos DM, Pereira JH, Dias MVB, Silva RG, Mendes MA, Palma MS, Basso LA, Santos DS (2003) Structural basis for inhibition of human PNP by immucillin-H. Biochem Biophys Res Commun 309:917–922

Deng H, Lewandowicz A, Schramm VL, Callender R (2004) Activating the phosphate nucleophile at the catalytic site of purine nucleoside phosphorylase: a vibrational spectroscopic study. J Am Chem Soc 126:9516–9517

Deng H, Murkin AS, Schramm VL (2006) Phosphate activation in the ground state of purine nucleoside phosphorylase. J Am Chem Soc 128:7765–7771

Doskocil J, Holy A (1977) Specificity of purine nucleoside phosphorylase from *Escherichia coli*. Collection Czechoslov Chem Commun 42:370–383

Ealick SE, Rule SA, Carter DC, Greenhough TJ, Babu YS, Cook WJ, Habash J, Helliwell JR, Stoeckler JD, Parks RE Jr, Chen S, Bugg CE (1990) Three-dimensional structure of human erythrocytic purine nucleoside phosphorylase at 3.2 Å resolution. J Biol Chem 265:1812–1820

Erion MD, Takabayashi K, Smith HB, Kessi J, Wagner S, Hönger S, Shames SL, Ealick SE (1997a) Purine nucleoside phosphorylase. 1. Structure-function studies. Biochemistry 36:11725–34

Erion MD, Stoeckler JD, Guida WC, Walter L, Ealick SE (1997b) Purine nucleoside phosphorylase. 2. Catalytic mechanism. Biochemistry 36:11735–11748

Frey PA, Sammons RD (1985) Bond order and charge localization in nucleoside phosphorothioates. Science 228:541–545

Frey PA (1989) Chiral phosphorothioates: stereochemical analysis of enzymatic substitution at phosphorus. Adv Enzymol Relat Areas Mol Biol 62:119–201

Gerlt JA, Demou PC, Mehdi S (1982) Oxygen-17 NMR spectral properties of simple phosphate esters and adenine nucleotides. J Am Chem Soc 104:2848–2856

Golos B, Dzik JM, Kazimierczuk Z, Ciesla J, Zielinski Z, Jankowska J, Kraszewski A, Stawinski J, Rode W, Shugar D (2001) Interaction of thymidylate synthase with the 5′-thiophosphates, 5′-dithiophosphates, 5′-H-phosphonates and 5′-S-thiosulfates of 2′-deoxyuridine, thymidine and 5-fluoro-2′-deoxyuridine. Biol Chem 382:1439–1445

Hendler SS, Fuerer E, Srinivasan PR (1970) Synthesis and chemical properties of monomers and polymers containing 7-methylguanine and an investigation of their substrate or template properties for bacterial deoxyribonucleic acid or ribonucleic acid polymerases. Biochemistry 9:4141–4153

Jaffe EK, Cohn M (1978) ^{31}P nuclear magnetic resonance spectra of the thiophosphate analogs of adenine nucleotides; effects of pH and Mg^{2+} binding. Biochemistry 17:652–657

Jensen KF, Nygaard P (1975) Purine nucleoside phosphorylase from *Escherichia coli* and *Salmonella typhimurium.* Purification and some properties. Eur J Biochem 51:253–265

Jensen KF (1976) Purine nucleoside phosphorylase from *Escherichia coli* and *Salmonella typhimurium.* Initial velocity kinetics, ligand binding and reaction mechanism. Eur J Biochem 61:377–386

Jungas RL (2006) Best literature values for the pK of carbonic and phosphoric acid under physiological conditions. Anal Biochem 349:1–15

Kicska GA, Tyler PC, Evans GB, Furneaux RH, Shi W, Fedorov A, Lewandowicz A, Cahill SM, Almo SC, Schramm VL (2002) Atomic dissection of the hydrogen bond network for transition-state analogue binding to purine nucleoside phosphorylase. Biochemistry 41:14489–14498

Kierdaszuk B, Modrak-Wójcik A, Shugar D (1997) Binding of phosphate and sulfate anions by purine nucleoside phosphorylase from *E coli*: ligand dependent quenching of enzyme intrinsic fluorescence. Biophys Chem 63:107–118

Kierdaszuk B, Modrak-Wójcik A, Wierzchowski J, Shugar D, (2000) Formycin A and its N-methyl analogues, specific inhibitor of *E coli* purine nucleoside phosphorylase (PNP): induced tautomeric shifts on binding to enzyme, and enzyme-ligand fluorescence resonance energy transfer. Biochim Biophys Acta 1476:109–128

Kline PC, Schramm VL (1992) Purine nucleoside phosphorylase. Inosine hydrolysis, tight binding of the hypoxanthine intermediate, and third-the-sites reactivity. Biochemistry 31:5964–5973

Kline PC, Schramm VL (1995) Pre-steady-state transition-state analysis of the hydrolytic reaction catalyzed by purine nucleoside phosphorylase. Biochemistry 34:1153–1162

Koellner G, Luić M, Shugar D, Seanger W, Bzowska A (1997) Crystal structure of calf spleen purine nucleoside phosphorylase in a complex with hypoxanthine at 2.15 Å resolution. J Mol Biol 265:202–216

Koellner G, Luić M, Shugar D, Seanger W, Bzowska A (1998) Crystal structure of the ternary complex of *E coli* purine nucleoside phosphorylase with formycin B, a structural analogue of the substrate inosine, and phosphate (sulphate) at 2.1 Å resolution. J Mol Biol 280:153–166

Koellner G, Bzowska A, Wielgus-Kutrowska B, Luić M, Steiner T, Seanger W, Stępiński J (2002) Open and closed conformation of the *E coli* purine nucleoside phosphorylase active center and implications for the catalytic mechanism. J Mol Biol 315:351–371

Koshland DE, Némethy G, Filmer D (1966) Comparison of experimental binding data and theoretical models in proteins containing subunits. Biochemistry 5:365–385

Krenitsky TA, Tuttle JV, Miller WH, Moorman AR, Orr GF, Beauchamp L (1990) Nucleotide analogue inhibitors of purine nucleoside phosphorylase. J Biol Chem 265:3066–3069

Kulikowska E, Bzowska A, Holy A, Magnowska L, Shugar D (1998) Antiviral acyclic nucleoside phosphonate analogues as inhibitors of purine nucleoside phosphorylases. Adv Exp Med Biol 431:747–752

Lewandowicz A, Schramm VL (2004) Transition state analysis for human and *Plasmodium falciparum* purine nucleoside phosphorylases. Biochemistry 43:1458–1468

Mao C, Cook WJ, Zhou M, Koszalka GW, Krenitsky TA, Ealick SE (1997) The crystal structure of *E coli* purine nucleoside phosphorylase: a comparison with human enzyme reveals a conserved topology. Structure 5:1373–1383

Mao C, Cook WJ, Zhou M, Federov AA, Almo SC, Ealick SE (1998) Calf spleen purine nucleoside phosphorylase complexed with substrates and substrate analogues. Biochemistry 37:7135–7146

Modrak-Wójcik A, Stępniak K, Akoev V, Żółkiewski M, Bzowska A (2006) Molecular architecture of *E. coli* purine nucleoside phosphorylase studied by analytical ultracentrifugation and CD spectroscopy. Protein Sci 15:1794–1800

Naito Y, Lowenstein JM (1985) 5′-Nucleotidase from rat heart membranes. Inhibition by adenine nucleotides and related compounds. Biochem J 226:645–651

Narayana SVL, Bugg CE, Ealick SE (1997) Refined structure of purine nucleoside phosphorylase at 2.75 Å resolution. Acta Crystallog D 53:131–142

Neet KE (1980) Cooperativity in enzyme function: equilibrium and kinetic aspects. Methods Enzymol 64:139–192

Pugmire MJ, Ealick SE (2002) Structural analyses reveal two distinct families of nucleoside phosphorylases. Biochem J 361:1–25

Ropp PA, Traut TW (1991) Purine nucleoside phosphorylase. Allosteric regulation of a dissociating enzyme. J Biol Chem 266:7682–7687

Sauve AA, Cahill SM, Zech SG, Basso LA, Lewandowicz A, Santos DS, Grubmeyer Ch, Evans GB, Furneaux RH, Tyler PC, McDermott A, Girvin ME, Schramm VL (2003) Ionic states of substrates and transition state analogues at the catalytic sites of *N*-ribosyltransferases. Biochemistry 42:5694–5705

Schnick C, Robien MA, Brzozowski AM, Dodson EJ, Murshudov GN, Anderson L, Luft JR, Mehlin C, Hol WG, Brannigan JA, Wilkinson AJ (2005) Structures of *Plasmodium falciparum* purine nucleoside phosphorylase complexed with sulfate and its

natural substrate inosine. Acta Crystallogr D Biol Crystallogr 61:1245–1254

Stoeckler JD, Agarwal RP, Agarwal KC, Schmid K, Parks RE Jr (1978a) Purine nucleoside phosphorylase from human erythrocytes: physicochemical properties of the crystalline enzyme. Biochemistry 17:278–283

Stoeckler JD, Agarwal RP, Agarwal KC, Parks RE Jr (1978b) Purine nucleoside phosphorylase from human erythrocytes. Methods Enzymol 51:530–538

Stoychev G, Kierdaszuk B, Shugar D (2001) Interaction of *Escherichia coli* purine nucleoside phosphorylase (PNP) with the cationic and zwitterionic forms of the fluorescent substrate *N*(7)-methylguanosine. Biochim Biophys Acta 1544:74–88

Stoychev G, Kierdaszuk B, Shugar D (2002) Xanthosine and xanthine. Substrate properties with purine nucleoside phosphorylases, and relevance to other enzyme systems. Eur J Biochem 269:4048–4057

Taylor Ringia EA, Schramm VL (2006) Transition states and inhibitors of the purine nucleoside phosphorylase family. Curr Top Med Chem 5:1237–1258

Traut TW (1994) Physiological concentration of purines and pyrimidines. Mol Cell Biochem 140:1–22

Tuttle JV, Krenitsky TA (1984) Effects of acyclovir and its metabolites on purine nucleoside phosphorylase. J Biol Chem 259:4065–4069

Wielgus-Kutrowska B, Tebbe J, Schröder W, Luić M, Shugar D, Seanger W, Koellner G, Bzowska A (1998) *Cellulomonas sp.* purine nucleoside phosphorylase (PNP). Comparison with human and *E. coli* enzymes. Adv Exp Med Biol 431:259–264

Wierzchowski J, Shugar D (1982) Luminescence studies of formycin, its aglycone, and their N-methyl derivatives: tautomerisation, sites of protonation and phototautomerism. Photochem Photobiol 35:445–458

Williams SR, Gekeler V, McIvor RS, Martin DW Jr (1987) A human purine nucleoside phosphorylase deficiency caused by a single base change. J Biol Chem 262:2332–2338

Wlodarczyk J, Stoychev Galitonov G, Kierdaszuk B (2004) Identification of the tautomeric form of formycin A in its complex with *E coli* purine nucleoside phosphorylase based on the effect of enzyme-ligand binding on fluorescence and phosphorescence. Eur Biophys J 33:377–385

Zhao Z (1996) Thiophosphate derivatives as inhibitors of tyrosine phosphatases. Biochem Biophys Res Commun 218:480–484